Formation of a Biomimetic, Liquid-Crystalline Hydrogel by Self-Assembly and Polymerization of an Ionic Liquid

Dolly Batra,[†,‡] Daniel N.T. Hay,[†,§] and Millicent A. Firestone*[,†,‡]

Materials Science Division and Center for Nanoscale Materials, Argonne National Laboratory, 9700 South Cass Avenue, Argonne, Illinois 60439

Received December 17, 2006. Revised Manuscript Received May 17, 2007

Preparation and polymerization of a methylimidazolium-based ionic liquid (IL) that incorporates an acryloyl moiety at the terminus of a C_8 alkyl chain is described. The IL monomer weakly self-assembles upon addition of water and oligomerizes on mild heating. Initiator-free polymerization (as evidenced by FT-IR spectroscopy) can be achieved by UV irradiation, forming an elastic, self-supporting hydrogel. Small-angle X-ray scattering (SAXS) studies on the unsupported polymer demonstrate that the hydrogel adopts an ordered lamellar structure. The polymer can absorb large quantities of water, swelling to nearly 200 times its original volume and, in the process, becoming a highly disordered lamellar structure. Swelling studies conducted using a range of organic solvents demonstrate that the polymer can also be swollen (albeit to a lesser extent) by polar, hydrogen-bonding solvents such as ethanol.

Introduction

The development of responsive (i.e., exhibiting dramatic, reversible changes upon application of an external stimulus), nanostructured materials is expected to play a major role in nanoscience, allowing for the compartmentalization and spatial ordering of functional guests with control over their internal packing arrangement.[1−3] Synthetic polymer gels, consisting of an elastic, charged cross-linked network that can absorb a significant amount of water but not dissolve, represent one well-known class of responsive materials.[4] These polyelectrolytes can undergo substantial volume changes depending on their environment and thus have the potential to serve as materials for controlled drug release, artificial muscles, and sensors. To date, most of these polymer hydrogels, however, do not possess structural ordering in either the swollen or contracted state; rather, they are amorphous materials, in contrast to biological gels (e.g., connective tissue, cartilage, and cornea), which are known to adopt well-ordered structures and often show predictable stimuli-responsive properties.[5] Synthetic polymer hydrogels whose swelling and contraction are accompanied by predictable structural changes on the molecular and nanometer length scale could be used as the basis of responsive, biomimetic nanostructured materials comprising key components in "all-organic" devices in biomolecular electronics, photonics or solar energy conversion.[6,7]

Prior work by Osada and co-workers[8−11] has shown that polyelectrolyte gels with organized structures can be prepared by the introduction of cationic surfactants (e.g., *N*-alkylpyridinium ions) into, for example, polysulfonic networks.[12] More commonly, however, ordered hydrogels are prepared by the copolymerization of an *N*-alkylacrylate with acrylic acid.[13,14] Although the structural resemblance of many ionic liquids to conventional cationic surfactants has been noted previously,[15] little work has been directed toward adapting ILs as materials for nanostructured polymeric hydrogels. Several recent reports have described approaches for the preparation of nanostructured polymerized ILs. Many of these approaches have involved multistep syntheses to introduce various mesogenic groups into the ILs that promote the formation of liquid crystalline materials.[16−19] For ex-

* To whom correspondence should be addressed. Phone: 630-252-8298. Fax: 630-252-9151. E-mail: firestone@anl.gov.
† Materials Science Division, Argonne National Laboratory.
‡ Center for Nanoscale Materials, Argonne National Laboratory.
§ Current address: Nalco Company, Naperville, IL.

(1) Firestone, M. A.; Williams, D. E.; Seifert, S. *Nano Lett.* **2001**, *1*, 199−200.
(2) Laible, P. D.; Kelly, R. F.; Wasielewski, M. R.; Firestone, M. A. *J. Phys. Chem. B* **2005**, *109*, 23679−23686.
(3) Batra, D.; Varela, L. M.; Seifert, S.; Firestone, M. A. *Adv. Funct. Mater.* **2007**, *17*, 1279−1287.
(4) Osada, Y.; Gong, J. P. *Adv. Mater.* **1998**, *10*, 827−837.
(5) Elliott, G. F.; Hodson, S. A. *Rep. Prog. Phys.* **1998**, *61*, 1325−1365.
(6) Lester, C. L.; Smith, S. M.; Colson, C. D.; Guymon, C. A. *Chem. Mater.* **2003**, *15*, 3376−3384.
(7) Yerushalmi, R.; Scherz, A.; van der Boom, M. E.; Kraatz, H. B. *J. Mater. Chem.* **2005**, *15*, 4480−4487.
(8) Kaneko, T.; Nagasawa, H.; Gong, J. P.; Osada, Y. *Macromolecules* **2004**, *37*, 187−191.
(9) Kaneko, T.; Yamaoka, K.; Gong, J. P.; Osada, Y. *Macromolecules* **2000**, *33*, 4422−4426.
(10) Kaneko, T.; Yamaoka, K.; Gong, J. P.; Osada, Y. *Macromolecules* **2000**, *33*, 412−418.
(11) Shigekura, Y.; Chen, Y. M.; Furukawa, H.; Kaneko, T.; Kaneko, D.; Osada, Y.; Gong, J. P. *Adv. Mater.* **2005**, *17*, 2695−2699.
(12) Kim, B. S.; Ishizawa, M.; Gong, J. P.; Osada, Y. *J. Polym. Sci., Part A: Polym. Chem.* **1999**, *37*, 635−644.
(13) Uchida, M.; Kurosawa, M.; Osada, Y. *Macromolecules* **1995**, *28*, 4583−4586.
(14) Miyazaki, T.; Kaneko, T.; Gong, J. P.; Osada, Y.; Demura, M.; Suzuki, M. *Langmuir* **2002**, *18*, 965−967.
(15) Firestone, M. A.; Dzielawa, J. A.; Zapol, P.; Curtiss, L. A.; Seifert, S.; Dietz, M. L. *Langmuir* **2002**, *18*, 7258−7260.
(16) Kishimoto, K.; Yoshio, M.; Mukai, T.; Yoshizawa, M.; Ohno, H.; Kato, T. *J. Am. Chem. Soc.* **2003**, *125*, 3196−3197.
(17) Kishimoto, K.; Suzawa, T.; Yokota, T.; Mukai, T.; Ohno, H.; Kato, T. *J. Am. Chem. Soc.* **2005**, *127*, 15618−15623.
(18) Hoshino, K.; Yoshio, M.; Mukai, T.; Kishimoto, K.; Ohno, H.; Kato, T. *J. Polym. Sci., Part A: Polym. Chem.* **2003**, *41*, 3486−3492.
(19) Yoshio, M.; Kagata, T.; Hoshino, K.; Mukai, T.; Ohno, H.; Kato, T. *J. Am. Chem. Soc.* **2006**, *128*, 5570−5577.

10.1021/cm062992z CCC: $37.00
Published on Web 08/07/2007

ample, Ohno and co-workers modified an alkyl(methyl)-imidazolium salt to include a biphenyl mesogenic moiety and a polymerizable methacrylate end group.[18] Upon photopolymerization with a UV initiator, an anisotropic ion-conductive polymer formed with a smectic A phase. Koide and co-workers also used a biphenyl as a mesogen in the alkyl chain of an alkyl(vinyl)imidazolium monomer, which upon photopolymerization yielded a smectic E phase anisotropic ion-conducting polymer.[20] Most recently, Yoshio et al. described the synthesis of terminally functionalized acrylate fan-shaped imidazolium-based ILs that can be surface aligned and polymerized to form 1D ion conductors.[19] Although these polymers were ionic, in neither case was their swellability in either water or organic solvents evaluated. Muldoon and Gordon[21] however, demonstrated that the copolymerization of an alkylvinylimidazolium monomer with an alkyl(divinyl)imidazolium salt (with a cross-linking monomer), resulted in gel-type polymer beads that swelled in various organic solvents. The resultant material, however, lacked structural order, limiting its potential in several areas of application. Thus, significant opportunities exist in developing a self-assembly route for preparing materials that would combine the best properties afforded by polyelectrolyte hydrogels (responsiveness, large water reservoir), ionic liquids (thermal stability), and ordered nanostructures.

Herein, we describe the use of an IL monomer **not** incorporating a mesogenic group to form the basis of a nanostructured polymeric hydrogel. This work employs the self-assembly of a polymerizable analogue of 1-decyl-3-methylimidazolium chloride, $[C_{10}mim^+][Cl^-]$, which can adopt a wide range of self-assembled architectures (e.g., 1D lamellae, 2D hexagonal, and 3D cubic phases) upon addition of water.[22] The polymerizable moiety is introduced at the alkyl chain terminus as an acryloyl group (1-(8-(acryloyloxy)octyl)-3-methylimidazolium chloride, $[AcrC_8mim^+][Cl^-]$). Photopolymerization of the self-assembled monomeric amphiphiles is described, and the structure, thermal properties, and isothermal swelling and deswelling characteristics of the polymer gel are detailed.

Experimental Section

Unless otherwise noted, all reagents were purchased from Sigma-Aldrich (Milwaukee, WI) and used as received.

Synthesis of $[AcrC_8mim^+][Cl^-]$ and poly$[AcrC_8mim^+][Cl^-]$. *8-Chlorooctylacrylate (**3**).* To a solution of 8-chlorooctanol (10.0 g, 60.7 mmol) and acryloyl chloride (5.93 mL, 72.9 mmol) in CH_3CN (250 mL) was added triethylamine (10 mL, 72.9 mmol) at 0 °C over a period of 20 min. The reaction mixture was allowed to warm to room temperature and then stirred for 18 h. It is noted that these reaction conditions serve to reduce the amount of polymerized 8-chlorooctylacrylate while providing acceptable yields for the title monomer. The resulting precipitate was removed by filtration, and the filtrate was reduced in vacuo. The residue was quenched with dilute HCl (1N, 200 mL), and the crude product was extracted from the mixture with ethyl acetate (3 × 100 mL). The organic layers were combined, dried (Na_2SO_4), and reduced in vacuo. The crude residue was distilled under reduced pressure (125−130 °C, 2 mmHg) to yield a colorless oil (11.5 g, 87%): ^{1}H NMR (500 MHz, $CDCl_3$) δ 6.38−6.42 (dd, J = 17.3, 1.5, 1H), 6.09−6.15 (dd, J = 17.3, 10.4, 1H), 5.81−5.83 (dd, J = 10.4, 1.5, 1H), 4.14−4.17 (t, J = 6.7, 2H), 3.53 (t, J = 6.7, 2H), 1.75 − 2.04 (m, 2H), 1.65−1.68 (m, 2H), 1.25−1.45 (m, 8H); ^{13}C NMR (125 MHz, $CDCl_3$) δ 166.4, 130.6, 128.7, 64.7, 45.2, 32.7, 29.2, 28.8, 28.6, 26.9, 25.9; ATR-IR 2928, 2855, 1725, 1464, 1190, 1059, 810 cm^{-1}. LRMS (ESI) *m/z* calcd for $C_{11}H_{19}ClO_2$ [M + Na$^+$], 241.1. Found, 241.1.

*1-(8-(Acryloyloxy)octyl)-3-methylimidazolium chloride, [Acr-C_8mim$^+$][Cl$^-$] (**5**).* A mixture of 8-chlorooctylacrylate (11.4 g, 51.9 mmol) and 1-methylimidazole (20.7 mL, 259 mmol) was heated to 85 °C and stirred for 18 h. Upon being cooled to RT, the reaction mixture was found to phase separate. The entire mixture was washed with ethyl acetate (3 × 50 mL) to remove any remaining starting material. The crude residue, a mixture of the title compound and polymerized side product, was reduced in vacuo and separated and purified via silica gel column chromatography (20% MeOH in CH_3CN). The purified product was taken up in CH_3CN and separated from the SiO_2 by filtration as a means to remove any coeluted silica in the final purified product The residue was reduced in vacuo to yield a waxy white solid (4.0 g, 26%): ^{1}H NMR (500 MHz, CD_3CN) δ 9.51 (s, 1H), 7.46 (t, J = 1.8 , 1H), 7.43 (s, J = 1.7, 1H), 6.29 − 6.33 (dd, J = 17.3, 1.5, 1H), 6.09 − 6.14 (dd, J = 17.3, 10.4 1H), 5.82 − 5.84 (dd, J = 10.4, 1.5, 1H), 4.17 (t, J = 7.3, 2H), 4.09 (t, J = 6.7, 2H), 3.87 (s, 3H), 1.80 − 1.85 (m, 2H), 1.59 − 1.64 (m, 2H), 1.30 − 1.36 (m, 8H); ^{13}C NMR (125 MHz, CD_3CN)) δ 166.9, 137.9, 131.2, 129.5, 124.4, 123.0, 65.2, 50.2, 36.7, 30.6, 29.6, 29.4, 29.2, 26.5, 26.3; ATR-IR 3437, 3090, 3057, 2932, 2859, 1709, 1572, 1477, 1298, 1175, 858, 820, 799 cm^{-1}. LRMS (ESI) *m/z* calcd for $C_{15}H_{25}ClN_2O_2$ [M − Cl]$^{-+}$, 265.2. Found 265.1. Stable storage of the monomer can be achieved in the dark at −30 °C.

Poly(1-(8-(acryloyloxy)octyl)-3-methylimidazolium chloride), Poly[AcrC_8mim$^+$][Cl$^-$]. In a 1/2 dram vial, water (20 μL) was added to 1-(8-acrylodecyl)-3-methylimidazolium chloride (100.7 mg). (The initial water content of the starting monomer was 8% w/w as measured by TGA, making the total calculated aqueous content 23% w/w.) The tightly capped vial was heated at ∼60 °C and vortex mixed until a homogeneous mixture was obtained. A portion of the hot mixture was loaded into borosilicate glass pipettes (∼2−3 in.) using negative pressure. The pipet was allowed to cool to RT and clipped from its wider end. The sample was placed approximately 6 in. away from a high-intensity UV light source (Hanovia 400 W Mercury Arc Lamp) and irradiated for 2 h. The resulting polymer was removed from the pipet by breaking the pipet glass with a razor blade.

The extent of monomer to polymer conversion was determined by ^{1}H NMR.[23] Briefly, a photopolymerized polymer of known weight was Soxhlet extracted in ethanol to reclaim any residual, unreacted monomer. The ethanol was taken to dryness by rotary evaporation and the remaining residue solubilized in MeCN-d_3. A known quantity of the sample was spiked with a ferrocene standard and transferred to a 5 mm NMR tube. The ratio of the number of protons from the monomer (as indicated by the amount of C-2 protons (from the carbon between the two nitrogen atoms in the imidazolium ring) to ferrocene (4.1 ppm) in the ^{1}H NMR spectrum (using spectrometer integration values) were used to estimate the number of moles of recovered monomer.

Equilibrium Swelling in Various Solvents. Freshly synthesized poly$[AcrC_8mim^+][Cl^-]$ was cut into twelve cylindrical pieces with the dimensions 0.22 cm × 0.09 cm (L × W). Each piece was then

(20) Yoshizawa, H.; Mihara, T.; Koide, N. *Liq. Cryst.* **2005**, *32*, 143−149.
(21) Muldoon, M. J.; Gordon, C. M. *J. Polym. Sci., Part A: Polym. Chem.* **2004**, *42*, 3865−3869.
(22) Firestone, M. A.; Rickert, P. G.; Seifert, S.; Dietz, M. L. *Inorg. Chim. Acta* **2004**, *357*, 3991−3998.
(23) MacDonald, R. T.; Pulapura, S. K.; Svirkin, Y. Y.; Gross, R. A.; Kaplan, D. L.; Akkara, J.; Swift, G.; S., W. *Macromolecules* **1995**, *28*, 73−78.

Scheme 1

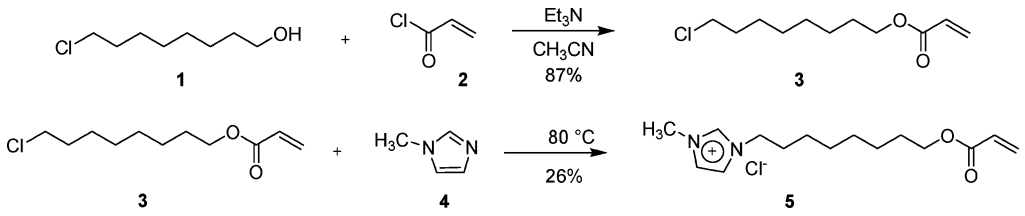

fully immersed into one of the following solvents: hexanes, ethyl acetate, octanol, chloroform, acetonitrile, dimethyl formamide (DMF), ethanol, dimethyl sulfoxide (DMSO), methanol, ethylene glycol, glycerol, or water. After 24 h, the samples were removed from the solvent and placed on a paper towel to remove excess solvent, and their lengths and widths were measured. The volume of the sample was calculated and a ratio of the final swelled volume (V_f) vs the initial volume (V_0) of the sample was determined (V/V_0). All measurements were made under ambient laboratory conditions: 21 °C (± 1 °C), 53% (± 3%) relative humidity.

Swelling−Deswelling Kinetics in Ethanol and Water. Freshly synthesized poly[$AcrC_8mim^+$][Cl^-] was cut into 0.45 cm × 0.09 cm and 0.50 cm × 0.09 cm (L × W) cylindrical pieces and fully immersed in water. The same polymer was also cut into 1.13 cm × 0.09 cm and 1.00 cm × 0.09 cm (L × W) cylindrical pieces and fully immersed in absolute ethanol. At periodic intervals, the samples were removed from the solvent and placed on a paper towel to remove excess solvent, and their lengths and widths were measured. For the polymer deswelling study, the fully swollen cylinders were placed on a paper towel and the length and width were again measured at periodic intervals. At each time interval (either solvent uptake or exclusion), the volume of the sample was calculated and a ratio of the volume at particular time interval (V_t) to the initial volume (V_0) of the sample was determined (V_t/V_0). All measurements were made at ambient laboratory conditions: 21 °C (± 1 °C), 53% (± 3%) relative humidity.

Physical Methods. All NMR experiments were performed on a Bruker model DMX 500 NMR spectrometer (11.7 T) equipped with a three-channel, 5 mm inverse detection, three-axis-gradient, variable-temperature probe with ^2H lock at 76.773 MHz. With the use of the nitrogen precooler, heater coil, and the variable temperature controller, the temperature was maintained at 295 K. Mass spectrometry was performed on a nanoflow (0.5 μL/min) Q Star XL TOF mass spectrometer equipped with electrospray ionization. A source voltage of 2000 V was empolyed. ATR/FT-IR spectroscopy was performed using a Bruker Vertex 70 spectrometer over the frequency range 4000−650 cm^{-1}. Spectra were recorded at 4 cm^{-1} resolution and averaged over 16 scans. Thermogravimetric analysis (TGA) was carried out on a TA instruments Q50 instrument by heating a known amount of sample (2−5 mg) in a Pt pan from 15 to 600 °C at a rate of 10 °C/min under a N_2 flow. For TGA kinetic studies, selected heating rates were examined (2, 5, 10, or 20 °C/min). The decomposition onset (T_{onset}) was calculated by extending the predegradation portion of the curve to the point of interception of the tangent line of the steepest portion of the mass curve during degradation. Differential scanning calorimetry (DSC) was performed on a TA instruments Q100 interfaced with a refrigerated cooling system. Instrument calibration was performed using an indium standard. Weighed amounts (1−5 mg) of samples were sealed in aluminum pans and equilibrated at −75 °C for 5 min prior to starting the heating/cooling cycle collected at 2 °C/min.

Small-angle X-ray scattering, SAXS, measurements were made using the instrument at undulator beamline 12ID-C (11−12 keV) of the Advanced Photon Source at Argonne National Laboratory. The 2D scattering profiles were recorded with either a MAR-CCD-165 detector (Mar USA, Evanston, IL), which features a circular, 165 mm diameter active area and 2048 × 2048 pixel resolution, or a custom-built mosaic detector (gold) consisting of 9 CCD chips with an image area of 15 × 5 cm^2 and 1536 × 1536 pixel resolution. The sample-to-detector distance was such as to provide a detecting range for momentum transfer of 0.0025 $Å^{-1} < q < 0.6$ $Å^{-1}$. The scattering vector, q, was calibrated using a silver behenate standard at $q = 1.076$ $Å^{-1}$. The 2D scattering images were first corrected for spatial distortion and sensitivity of the detector and then radially averaged to produce plots of scattered intensity, $I(q)$, versus scattering vector, q, where is $q = 4\pi/\lambda(\sin\theta)$. The value of q is proportional to the inverse of the length scale, $Å^{-1}$. For these measurements, samples were probed either as freely suspended polymers or as the gels confined in glass capillaries. Measurements were made at 25 °C (± 1 °C) and 24% (± 2%) relative humidity.

Results and Discussion

The synthesis of the ionic liquid (IL) monomer, [$AcrC_8mim^+$][Cl^-] (**5**), was carried out through a two step procedure (Scheme 1). First, the polymerizable "tail" of the IL was synthesized by coupling acryloyl chloride (**2**) with 8-chloro-1-octanol (**1**) using triethylamine as the base, giving 8-chlorooctylacrylate (**3**) in 87% yield. In the second step, 1-methylimidazole (**4**) was coupled with acrylate **3**. Because a high temperature (80 °C) was necessary to perform the latter (substitution) reaction, a significant amount of oligomerized starting material was found along with the final product, [$AcrC_8mim^+$][Cl^-] (**5**), which was isolated in a modest 26% yield after column chromatography. The purified product was a waxy solid that typically contains 8% (± 1%) (w/w) residual water, as measured by thermogravimetric analysis (Figure 4).

Attempts to increase the overall yield of **5** by performing the acylation after quarternization, it should be noted, resulted in significant oligomerization/polymerization (at 0 °C). When acylation was performed at a lower temperature (−20 °C), the product was often found to be contaminated with triethylammonium chloride, which is difficult to separate from the imidazolium chloride monomer **5**. High product purity is crucial for monomer self-assembly. Therefore, despite its low yield, the synthetic route outlined in Scheme 1 is preferable to alternate procedures yielding a greater quantity of lower purity [$AcrC_8mim^+$][Cl^-] (**5**).

DSC heating/cooling scans collected on monomer **5** over a wide range (−70 °C → 200 °C) show several endo- and exothermic phase transitions (Figure 1A). Specifically, the heating profile on the monomer shows a weak exothermic transition at −4 °C, which is a cold crystallization peak. Crystallization upon heating is common thermal behavior observed for ionic liquids and polymeric or amorphous compounds.[24] Next, a large endothermic transition at 34 °C

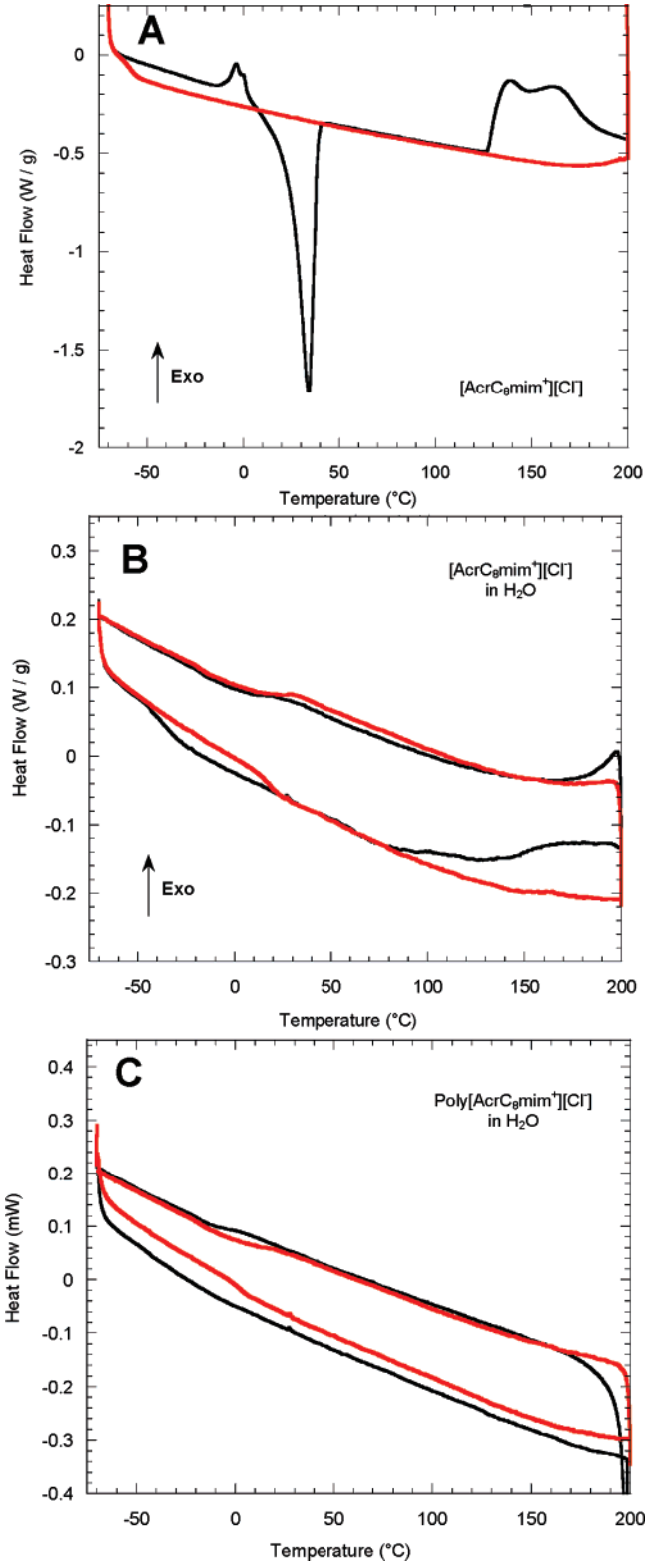

Figure 1. (A) DSC heating scan collected on freshly synthesized [$AcrC_8mim^+$][Cl^-] monomer with an initial water content of 8% (w/w) (black curve) and second heating scan collected on the exact same sample (red curve). (B) DSC heating and cooling curves obtained on binary mixture of [$AcrC_8mim^+$][Cl^-] and 21% (w/w) water (black curve) and second cycle collected on the exact same sample (red curve). (C) DSC heating and cooling curves for poly[$AcrC_8mim^+$][Cl^-] with a total water content of 15% (w/w) (black) and second cycle collected on the exact same sample. All measurements made using a scan rate 2 °C/min.

is observed and is the melting-point transition, in agreement with the observed waxy solid consistency of the sample at room temperature and the formation of a liquid upon heating.

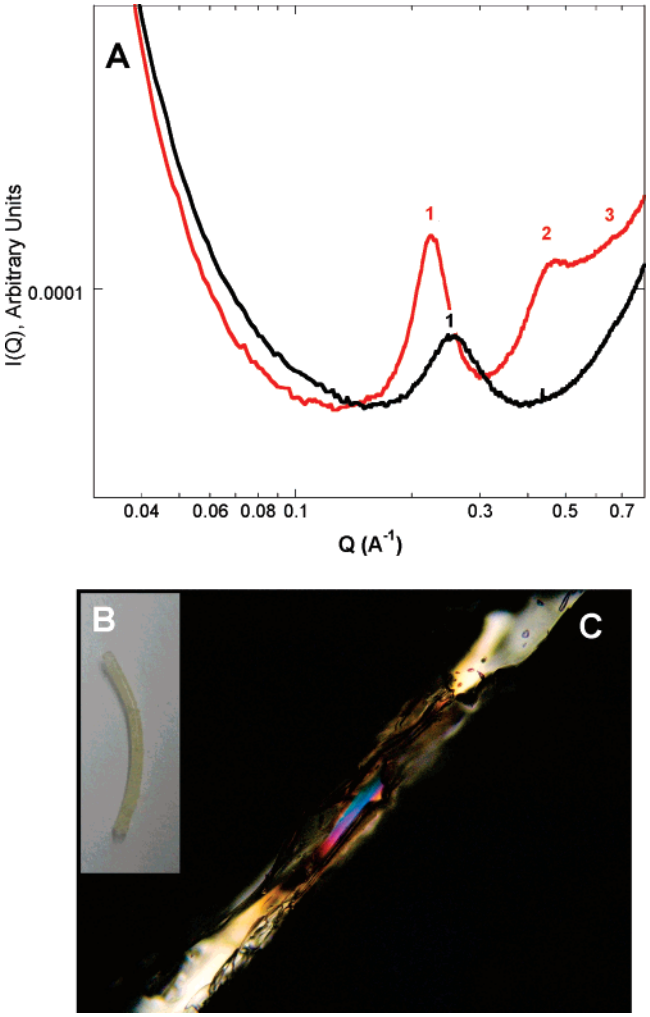

Figure 2. (A) Averaged small-angle X-ray scattering (SAXS) measurements collected on binary mixture of [$AcrC_8mim^+$][Cl^-] and 21% (w/w) water (black curve) and on poly[$AcrC_8mim^+$][Cl^-] (red curve). (B) Digital photograph of freshly synthesized poly[$AcrC_8mim^+$][Cl^-] after release from a glass capillary. (C) Representative polarized optical micrograph (10×) of poly[$AcrC_8mim^+$][Cl^-].

Further heating reveals a broad complex exothermic feature with two resolvable maxima at 139 and 165 °C. A second heating scan performed on the same sample (Figure 1A) shows a featureless thermogram, suggesting that thermal polymerization of the acrylate monomer has occurred. Thus, the high-temperature exotherm(s) observed during the first heating cycle most likely reflect the onset of thermal polymerization of the acrylate monomer.

Self-assembly of the amphiphilic monomer, [$AcrC_8mim^+$][Cl^-], was achieved by the addition of water to yield a total water content of 22 ± 3% (w/w). The mixture is a transparent, homogeneous, slightly viscous liquid (weak gel). The introduction of an appropriate amount of water promotes the formation of a weakly ordered material, as evidenced both by very weak optical birefringence when examined under polarized light and a single broad diffraction feature in the SAXS at $q = 0.257$ Å^{-1} (Figure 2A). The lack of appreciable structural ordering induced by the addition of water is in contrast with prior observations for alkylmeth-

(24) Fredlake, C. P.; Crosthwaite, J. M.; Hert, D. G.; Aki, S. N. V. K.; Brennecke, J. F. *J. Chem. Eng. Data* **2004**, *49*, 954−964.

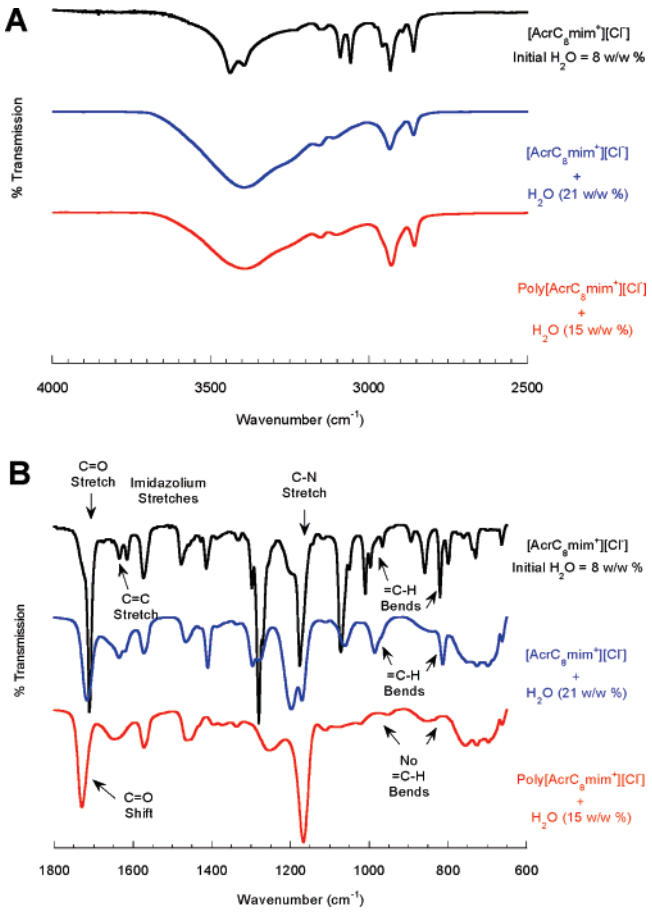

Figure 3. ATR-IR spectra of [$AcrC_8mim^+$][Cl^-], a homogeneous binary mixture of [$AcrC_8mim^+$][Cl^-] and water, and poly[$AcrC_8mim^+$][Cl^-] in the 4000−2500 cm^{-1} region (A), and 1800−650 cm^{-1} region (B).

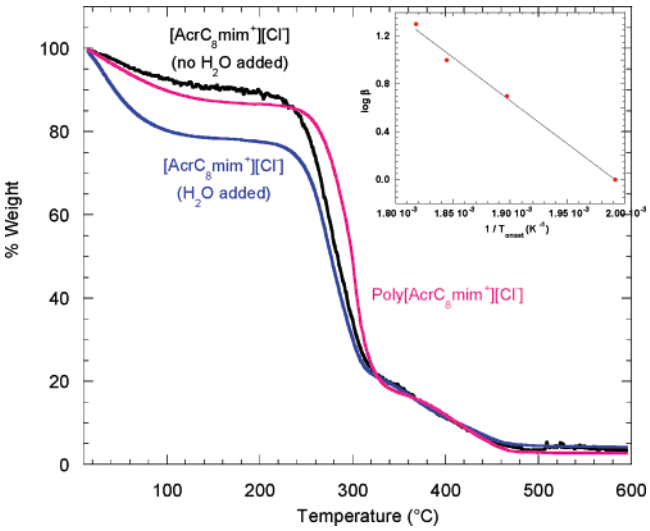

Figure 4. Representative TGA curves for as-synthesized 2−6 mg of [$AcrC_8mim^+$][Cl^-], a homogeneous mixture of [$AcrC_8mim^+$][Cl^-] in water, and poly[$AcrC_8mim^+$][Cl^-] synthesized by [$AcrC_8mim^+$][Cl^-] in 21% water (w/w). Water content was determined as the percentage of water lost from room temperature to 150 °C. The onset of decomposition (T_{onset}) was calculated by extending the pre-degradation portion of the curve after initial water loss to the point of interception of the tangent line of the steepest portion of the mass curve during degradation. Inset shows the Arrhenius plot of poly[$AcrC_8mim^+$][Cl^-] degradation determined at selected TGA heating rates. β is the heating rate (K min^{-1}) and T is T_{onset} (K) at $\beta = 1$, 2, 5, 10, and 20 K/min. Slope of the best line fit was determined to be -7.25×10^3 K.

ylimidazolium-based ILs.[22] That is, for [$C_{10}min^+$][Cl^-], strong birefringence and increased diffraction peaks in the SAXS pattern are observed upon the controlled addition of water. The inability to trigger the formation of a well-ordered mesophase upon addition of water here suggests that the acryloyl group inhibits the self-assembly of the ILs. This notion is supported by infrared investigations of headgroup interactions (Figure 3A). That is, prior work on the nonpolymerizable forms of this IL (decylmethylimidazolium ILs) showed that self-assembly and gelation arise from maintaining hydrogen-bonding interactions between the IL cation, bridging water, and the IL anion.[15,22] Similar studies conducted on acrylate IL water binary mixtures show preservation of the expected shifts of both the aromatic C−H stretching (3156 cm^{-1}), and the aromatic C−H hydrogen-bonded to the chloride anion (C−H···Cl^-) (3110 cm^{-1}). The observation of the anticipated modes confirms the partial disruption of the hydrogen bonding between the C−H of the imidazolium ring and the chloride anion by water, important bonding interactions that are believed to contribute to the self-assembly and gelation of the IL−water mixtures. Alternatively, the other important component, van der Waals interactions/packing of the alkyl chains, which promotes an ordered material, may be inhibited upon the introduction of the terminal acryloyl moiety.

DSC studies on the binary mixture also confirm the loss of crystallinity in the sample. Specifically, the heating and cooling thermograms show only the complex, broad, high-temperature exotherm with an onset at ca. 143 °C (Figure 1B) and the lack of the two low-temperature primary transitions arising from cold crystallization and melting. The loss of the melting transition is consistent with the liquid form of the binary mixture in a glassy amorphous state.[15,22,25] The second cycle collected on the same sample also reveals the loss of the exothermic transition attributed to the thermal polymerization. Additional cycling of the sample produces a secondary phase transition at 1.3 °C (midpoint). Thus, the thermally polymerized binary mixture possesses only a single glass transition, T_g.

Photopolymerization (UV irradiation for 1.5−2 h; Scheme 2) of the ionic liquid monomer, [$AcrC_8mim^+$][Cl^-], yields a free-standing, translucent, elastic cylindrical rod upon release from the glass capillary (Figure 2B). The polymerization of self-assembled hydrated amphiphiles bearing acryloyl groups by direct UV irradiation has been recently reviewed.[26] Also noted is that the photopolymerization does not appear to be inhibited by the presence of oxygen, which may be in part due to the poor solubility coupled with slow diffusivity of oxygen in dialkylimidazolium ILs.[27] Further details regarding the polymerization of this monomer are currently under study in this Laboratory. Under polarized light, the polymer shows strong optical birefringence (Figure 2C), signaling an enhancement in the structural ordering induced by polymerization. The SAXS results (Figure 2A) are consistent with

(25) Rickert, P. G.; Antonio, M. R.; Firestone, M. A.; Kubatko, K. A.; Szreder, T.; Wishert, J. F.; Dietz, M. L. *J. Phys. Chem. B* **2007**, *111*, 4865−4692.
(26) Mueller, A.; O'Brien, D. F. *Chem. Rev.* **2002**, *102*, 727−757.
(27) Anthony, J. L.; Maginn, E. J.; Brennecke, J. F. *J. Phys. Chem. B* **2002**, *106*, 7315−7320.

Scheme 2

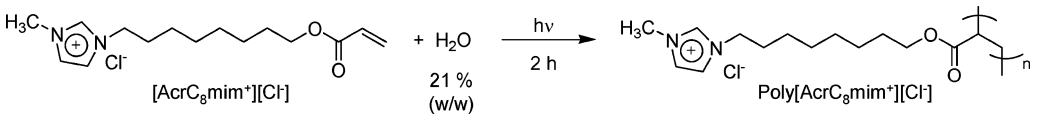

an increase in structural ordering, with three resolved Bragg diffraction peaks position at $q = 0.224$, 0.450, and 0.662 $Å^{-1}$. The integral ordering indexing with respect to the first-order peak clearly indicates that the polymer is an ordered lamellar structure with a lattice spacing of 28 Å.

Although the change in solution consistency (to a rubbery solid) is clearly indicative of polymerization of the IL cation, [$AcrC_8mim^+$], the actual extent of polymerization was confirmed by ATR/FT-IR spectroscopy (Figure 3). The polymerization process was followed by monitoring the vinyl C−H bending modes (998, 965, and 819 cm^{-1}) and the conjugated C═O stretching mode at 1710 cm^{-1} (Figure 3B).[28] (The C═C stretching mode at 1635 cm^{-1}, unfortunately, offers a poor diagnostic for polymerization, as it overlaps with the imidazolium stretches after the addition of water). Polymerization was also monitored by the loss of several signature modes of the acrylate group occurring at 1075 cm^{-1} (═CH_2 rocking mode), 1275 cm^{-1} (═CH rocking mode), and 1411 cm^{-1} (═CH_2 deformation).[29] The monomer−water mixture also exhibits shifts in the vinyl C−H bending modes to 986 and 812 cm^{-1} and a small upward shift of C═O stretch to 1717 cm^{-1}. These shifts may indicate partial polymerization of the monomer due to the heating/vortexing cycles necessary to prepare a uniform starting material. It is clear, however, that the bulk of the polymerization takes place after photochemical irradiation of the mixture for 2 h, evidenced by the complete disappearance of the vinyl C−H bending peaks, and a shift of the C═O stretch to the expected unconjugated mode positioned at 1731 cm^{-1}.[28] Moreover, as stated earlier, we find preservation of the hydrogen bond mediated assembly of the cation-bridging water-anion that serves to order the ILs.[15,22] Specifically, the 3156 and 3110 cm^{-1} peaks do not shift significantly after polymerization, suggesting that polymerization does not influence the assembly in the headgroup region (Figure 3A). Last, a high percentage of monomer to polymer conversion (98 ± 1 %) was determined via ^1H NMR spectroscopy.

Prior work by Tang et al. has demonstrated that methacryloyl-functionalized short chain dialkylimidazolium ILs can be thermally polymerized using an initiator (AIBN) to form unstructured polymers.[30,31] The use of a similar approach to thermally polymerize this IL monomer may also be possible, but preliminary studies of the effect of introducing an initiator to the binary mixture of IL monomer and water indicate that initiators alter the self-assembly. Therefore, this approach was not pursued. Thermal polymerization was attempted without the use of a radical initiator. However, thermal incubation of the mixture at 95 °C for up to 8 h does not appear to change the consistency of the gel. Indeed, an ATR/FT-IR spectrum of the heated product shows only slight polymerization, evidenced by a small decrease in the interactions of the vinyl C−H bends between 1000 and 800 cm^{-1} (data not shown).[28] Another ATR/FT-IR spectrum of the material after an ethanol wash to remove unreacted monomer, showed the same vinyl C−H bends, indicating that thermal incubation without an initiator results only in oligomerization of the IL monomer. This finding is in accord with the results from DSC, which clearly indicated that a higher temperature (>125 °C) was necessary to promote complete polymerization of the IL monomer in the absence of an initiator. This temperature is obviously well above the boiling point of water, a key component for the self-assembly of 1-methyl-3-decylimidazolium-derived ILs, rendering this approach impractical.

The thermal properties of the photopolymerized material, poly[$AcrC_8mim^+$][Cl^-], were determined by differential scanning calorimetry (DSC) and thermogravimetric analysis (TGA). As expected, the DSC thermogram (Figure 1C) is devoid of any first-order phase transitions over the experimental range studied, (−70 to 200 °C). A weak secondary phase transition, T_g, was observed in the heating scan with a midpoint positioned at 18 °C and was reversible upon cooling. Tang et al.[32] have shown that the T_g of poly(IL)s is highly dependent on the properties of the anion and the polycationic backbone; hence, the literature-reported T_g values for imidazolium-based poly(IL)s show a wide variation between −75 and 110 °C, with lower T_g values attainable for systems featuring longer alkyl chains because of increased polymer backbone flexibility.[32−34]

Thermogravimetric analysis indicates that the sample dehydrates upon polymerization, reducing the initial water content to well below that added to the form the binary mixture (15 ± 1% (w/w)) (Figure 4). In addition, the TGA data show that the polymer is slightly more thermally stable than the self-assembled monomer precursor solution. Specifically, the polymer shows a 24 °C increase (from 245 to 269 °C) in the decomposition onset temperature (T_{onset}). Both the monomer and polymer displayed multistep degradations with 5−10% residue remaining after 465 °C. Similar decomposition profiles for chemically crosslinked vinylimidazolium-polyIL have been reported by Muldoon and Gordon.[21]

The thermal decomposition can be further analyzed using the method of Flynn and Wall.[35] Specifically, the activation

(28) Pretsch, E.; Clerc, T.; Seibel, J.; Simon, W. *Tables of Spectral Data for Structure Determination of Organic Compounds*, 2nd English ed.; Springer-Verlag: New York, 1989.
(29) Colthup, N. B.; Daly, L. H.; Wiberley, S. E. *Introduction to Infrared and Raman Spectroscopy*; 3rd ed.; Academic Press: San Diego, 1990.
(30) Begam, T.; Tomar, R. S.; Nagpal, A. K.; Singhal, R. *J. Appl. Polym. Sci.* **2004**, *94*, 40−52.
(31) Tang, J. B.; Tang, H. D.; Sun, W. L.; Plancher, H.; Radosz, M.; Shen, Y. Q. *Chem. Commun.* **2005**, 3325−3327.
(32) Tang, J. B.; Tang, H. D.; Sun, W. L.; Radosz, M.; Shen, Y. Q. *J. Polym. Sci., Part A: Polym. Chem.* **2005**, *43*, 5477−5489.
(33) Yoshizawa, M.; Ohno, H. *Chem. Lett.* **1999**, 889−890.
(34) Ohno, H.; Yoshizawa, M.; Ogihara, W. *Electrochim. Acta* **2004**, *50*, 255−261.
(35) Flynn, J. H.; Wall, L. A. *Polym. Lett.* **1966**, *4*.

energy (E_a) of polymer decomposition can be determined by measuring T_{onset} at various heat rates. The E_a for a given polymer can then be determined by the following equation, assuming basic Arrhenius equation and first-order kinetics

$$E_a = \left(\frac{-R}{b}\right)\frac{d \log \beta}{d(1/T)} \quad (1)$$

Where R is the gas constant (8.314 J mol^{-1} K^{-1}), b is a constant (0.457), β is the heating rate (K min^{-1}) and T is T_{onset} (K) for the thermal decomposition. From the slope of a plot (Figure 4 insert) of log β versus $1/T_{onset}$ (collected at heat rates between 1 and 20 K/min), the activation energy for decomposition, E_a, was determined to be 132 kJ /mol (31.4 kcal/mol). This value is significantly higher than that observed for chemically similar amorphous homopolymers such as poly(methyl acrylate) and poly(methyl methacrylate) (95 kJ/mol).[36] Moreover, the E_a approaches that previously reported for certain side-chain polymer liquid crystals (SCPLCs), incorporating a polyacrylate backbone and a liquid-crystalline mesogenic core.[36] Thus, this result suggests that the liquid crystallinity and/or physical cross-linking in the acrylate IL polymer impart additional thermal stability.

Solvent Interactions. Poly[AcrC$_8$mim$^+$][Cl$^-$] was found to be maximally swollen in short-chain alcohols (e.g., methanol or ethanol) and water, producing colorless, optically transparent, self-supporting gels (Figure 5A). In contrast, poorly swollen polymers resulted after hexane or chloroform incubation, producing pale yellow, opaque materials (Figure 5A). The kinetics of polymer swelling and deswelling was studied by monitoring the volume change as a function of time in water and ethanol. Figure 5B shows the rate of solvent uptake by a freshly prepared poly[AcrC$_8$mim$^+$][Cl$^-$] sample determined by measuring the volume of the polymer at periodic intervals after immersion. The kinetic profiles show that equilibrium swelling of the polymer is achieved much faster in water (1 h) than ethanol (3 h). The swelling in both solvents shows a nonlinear increase, indicating the solvent transport mechanism to be a combination of diffusion and relaxation control.[37] The deswelling profiles were also found to decrease nonlinearly at room temperature under ambient conditions. This deswelling was found to proceed at a faster rate for ethanol than water, presumably due to the much lower boiling point of ethanol (78 °C) than water (100 °C). Specifically, complete polymer deswelling occurs in ~2.5 and ~30 h from ethanol and water, respectively.

The swelling and deswelling mechanisms can be compared to those of other polyelectrolyte gels, in which the repulsive forces of the fixed charges in the polymer network and the osmotic pressure of the mobile free counterions play significant roles.[38] The ability of water to contribute to both these forces in poly[AcrC$_8$mim$^+$][Cl$^-$] might explain the faster and higher extent of swelling in water than ethanol. Indeed, Volkov et al.[39] have shown that the counterion

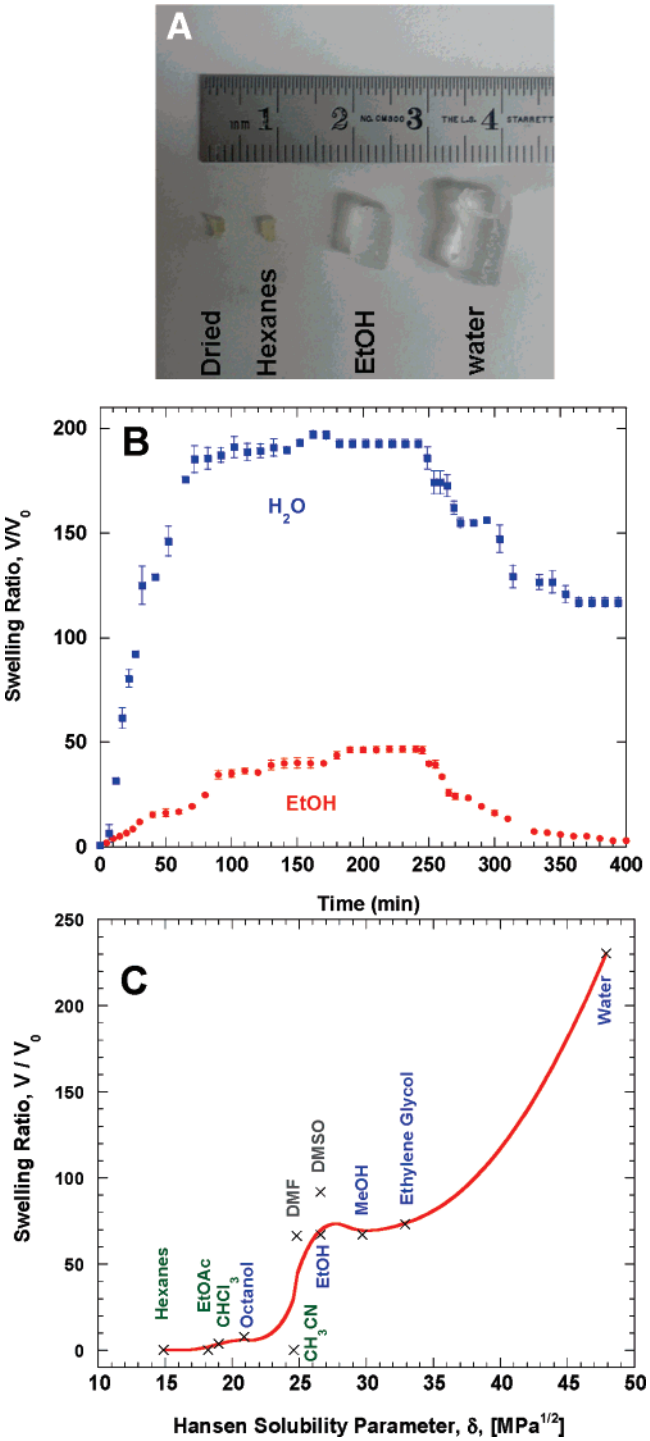

Figure 5. (A) Digital photographs of a small piece of poly[AcrC$_8$mim$^+$][Cl$^-$], and a similar sized poly[AcrC$_8$mim$^+$][Cl$^-$] swollen to equilibrium (24 h) in hexanes, ethanol, and water. (B) Volume changes of poly[AcrC$_8$mim$^+$][Cl$^-$] as a function of time during ethanol or water swelling and air deswelling (started at 240 min). (C) Equilibrium volume changes (V/V_o) of poly[AcrC$_8$mim$^+$][Cl$^-$] as a function of Hansen solubility parameter evaluated for a range of organic solvents and water after 24 h of incubation.

contributes to differing swelling processes in alcoholic versus aqueous solvents, with both free and bound counterions coexisting in the swelled state in methanol, but predominantly free counterions existing in water.

A more complete examination of the swelling characteristics of the polymer was carried out by determination of the equilibrium volume swelling ratio (V_f/V_o at t_f= 24 h) in solvents selected over a wide range of (Hansen) solubility

(36) Mano, J. F. *E-Polymers* **2004**, no. 077.
(37) Kabra, B. G.; Gehrke, S. H.; Hwang, S. T.; Ritschel, W. A. *J. Appl. Polym. Sci.* **1991**, *42*, 2409−2416.
(38) Kokufuta, E. *Langmuir* **2005**, *21*, 10004−10015.
(39) Volkov, E. V.; Fillippova, O. E.; Khokhlov, A. R. *Colloid J.* **2004**, *66*, 663−668.

parameters (Figure 5C). The Hansen solubility parameter (δ) is a three-dimensional solubility parameter dividing the total Hildebrand value into three parts, a dispersion force component, δ_d, a polar component (dipole−dipole), δ_p, and a hydrogen-bonding component, δ_h, which is given by

$$\delta^2 = \delta_d{}^2 + \delta_p{}^2 + \delta_h{}^2 \quad (2)$$

As shown in Figure 5C, the maximum swelling of the polymer (to ~250 times its original volume) is observed in water, with a δ value of 48 MPa $^{1/2}$ (23.5 cal$^{1/2}$ cm $^{-3/2}$). This provides an estimation of the solubility parameter for the polymer, because it has been previously established that the degree of swelling reaches a maximum when the polymer network is in a solvent of a similar solubility parameter (i.e., cohesive interactions).[40−42] Figure 5C indicates that, in general, with increasing polarity, the polymer solubility increases. More specifically, among the organic solvents examined, polar organics (e.g., short-chain alcohols, DMSO, and DMF) produce well-swollen polymers, whereas nonpolar solvents such as hexane yield minimally swollen materials. The role of hydrogen-bonding interactions can also be evaluated by examining the relative ability of the various solvents to participate in hydrogen bonding (roughly divided into poor (green), moderate (gray), or superior (blue), according to A. F. M. Barton[43]) as a function of the equilibrium swelling ratio (Figure 5C). Clearly, poor H-bonding solvents promote unfavorable interactions with the polymer network. The role of H-bonding can be further examined by plotting the equilibrium swelling ratio vs the individual hydrogen-bonding component of the Hansen solubility parameter, δ_h, (see the Supporting Information, Figure S7). Such a plot shows that solvents possessing a δ_h value of greater than 26.6 MPa$^{1/2}$ yield maximally swollen gels. A similar plot made considering only the dispersion force component of the Hansen solubility parameter, δ_d, (see the Supporting Information, Figure S6) does not yield any correlation with the solvents examined in this study, indicating that this component does not significantly contribute to the solubility/swelling of the polymer. The solubility characteristics of the poly[AcrC$_8$mim$^+$][Cl$^-$] compare favorably with the Hildebrand solubility parameters determined for 1-alkyl-3-methylimidazolium-based RTILs.[44] Prior work has determined that the solubility parameters for poly(alkyl)-acrylates, which show miscibility with weakly polar hydrogen-bonding solvents, are typically in the range of 16−25 MPa$^{1/2}$.[45] The observed swelling of poly(AcrC$_8$mim$^+$][Cl$^-$] in polar hydrogen-bonding solvents must therefore arise from preferential solvation of the imidazolium headgroup rather than poly(alkyl)acrylate backbone.

To further evaluate the swelling of the gel in water, we monitored the structural evolution of the water swollen gel by SAXS. Figure 6 compares the patterns collected on an unswollen polymer, after exposure to water for 1 h and postincubation in water for 24 h. The scattering curve collected on the fully swollen (24 h water) polymer shows two very broad features approximately positioned at $q \approx 0.03$ and 0.06 Å^{-1}, indicative of a highly disordered lamellar structure with a significantly increased d-spacing of ~209 Å. Increased structural ordering and a decrease in the interlamellar spacing ($d \sim 157$ Å) is observed in samples that have only been exposed to water of 1 h (Figure 6A). Finally, a fully contracted, nonswollen polymer shows a 7-fold decrease in the d-spacing to 28.5 Å. These studies indicate that the uptake of water simply serves to increase the bilayer separation (Figure 6B), most likely by increasing the thickness of the water layer. These findings support the solubility studies confirming that water solvation of the imidazolium headgroup drives the swelling of the polymer. More complete structural details monitoring the evolution of the polymer structure using complementary neutron scattering, a technique ideally suited for probing the water layer thickness, will be the focus of future work.

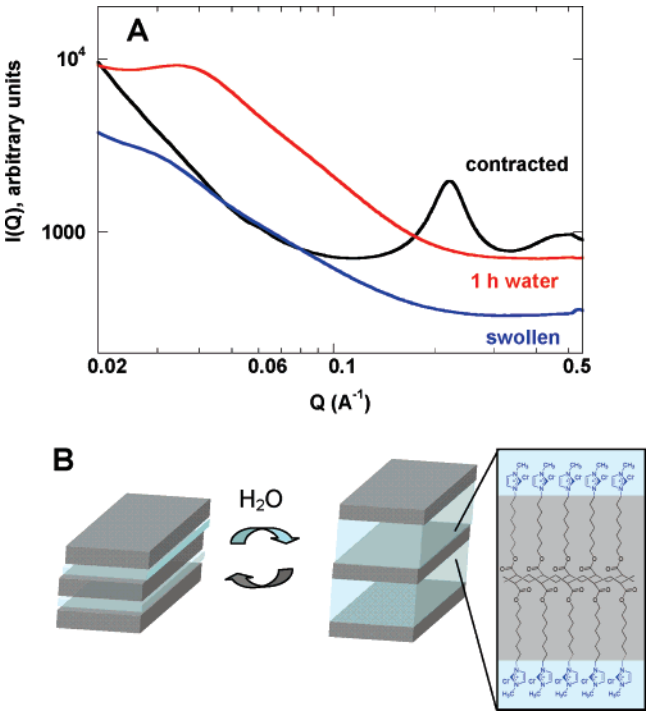

Figure 6. (A) Averaged SAXS data collected on a nonswollen poly[AcrC$_8$-mim$^+$][Cl$^-$], after 1 and 24 h of incubation in water. (B) Schematic illustration of proposed structure in the swollen and deswollen states.

Conclusions

We have developed a straightforward means by which to prepare a nanostructured, biomimetic hydrogel through self-assembly and photopolymerization of an ionic liquid acrylate monomer, [AcrC$_8$mim$^+$][Cl$^-$]. The monomer has been designed to incorporate molecular components that both promote its self-assembly (via water-mediated hydrogen-bonding interactions between the anion and cationic headgroup) and permit ready photopolymerization (via an acryloyl group) to covalently link the IL mesogens at the alkyl chain terminus. Unlike typical photopolymerized hydrated am-

(40) Okay, O.; Akkan, U. *Polym. Bull.* **1998**, *41*, 363−370.
(41) Lozano, P.; de Diego, T.; Gmouh, S.; Vaultier, M.; Iborra, J. L. *Biotechnol. Prog.* **2004**, *20*, 661−669.
(42) Mutelet, F.; Butet, V.; Jaubert, J. N. *Ind. Eng. Chem. Res.* **2005**, *44*, 4120−4127.
(43) Barton, A. F. M. *Chem. Rev.* **1975**, *75*, 731−753.
(44) Lee, S. H.; Lee, S. B. *Chem. Comm.* **2005**, 3469−3471.
(45) Grulke, E. A. In *Polymer Handbook*, 3rd ed.; Brandrup, J., Immergut, E. H., Eds.; Wiley-Interscience: New York, 1989.

phiphiles, the product is found to possess improved structural ordering vs the noncovalent preassembly, adopting a liquid-crystalline, lamellar (bilayer) structure. The polymer architecture resembles that of cellular environments, featuring amphiphilic bilayers separated by large water channels, thus offering the possibility of sequestering both lipophilic and water-soluble guests into the segregated domains. The resultant nanostructured hydrogel has been shown to have good thermal stability and is sufficiently physically cross-linked to undergo reversible swelling in water to more than 200 times its original contracted volume and 45 times its volume in polar hydrogen- bonding solvents such as short-chain alcohols. In addition, the amphiphilic nature of poly[AcrC_8mim$^+$][Cl$^-$] allows the polymer to swell not only in water but also other polymer hydrogen-bonding solvents, widening its potential for use in applications as a nanostructured organogel. The reversible swellability of the polymer and the inability to be solublized in organic solvents suggests cross-linking polymerization rather than linear polymerization.[26] Although in the fully water swollen state the lamellar structure becomes highly disordered, it does possess features in the SAXS pattern to indicate preservation of mutlibilayer structural ordering. The bilayer mesophase architecture and the ability to absorb large amounts of water with a concomitant increase in the interbilayer distance suggests the possible use of these materials as mechanically durable biomembrane mimics for the encapsulation of both water-soluble and membrane-bound biomolecules. Future studies will examine the stability and integration of both water-soluble and membrane proteins into the hydrogels and the use of the tunable mesophase architecture to regulate the internal packing arrangement of the encapsulated guests.

Acknowledgment. The authors thank Mr. Anthony Crisci for his assistance in preparing samples used for the SAXS studies and Dr. Sönke Seifert for his help with the SAXS experiments. This work was performed under the auspices of the Office of Basic Energy Sciences, Division of Materials Sciences, United States Department of Energy, under Contract DE-AC02-06CH11357.

Supporting Information Available: ^{1}H and ^{13}C spectra of 8-chlorooctylacrylate (**3**) and 1-(8-(acryloyloxy)octyl)-3-methylimidazolium chloride (**5**), and sample TGA curves of poly[AcrC_8mim$^+$][Cl$^-$] at various heat rates (used to determine E_a of polymer degradation) and swelling rations (V/V_o) plotted against Hansen dispersion and hydrogen-bonding parameters for selected solvents (PDF). This material is available free of charge via the Internet at http://pubs.acs.org.

CM062992Z